Electrochemical behavior of Neodymium and formation of Mg-Nd alloys in molten Chlorides

Hua, Zhongsheng; Liu, Huan; Wang, Jian; He, Jiwen; Xiao, Saijun; Xiao, Yanping; Yang, Yongxiang

DOI
10.1021/acssuschemeng.7b01708

Publication date
2017

Document Version
Final published version

Published in
ACS Sustainable Chemistry and Engineering

Citation (APA)
Hua, Z., Liu, H., Wang, J., He, J., Xiao, S., Xiao, Y., & Yang, Y. (2017). Electrochemical behavior of Neodymium and formation of Mg-Nd alloys in molten Chlorides. *ACS Sustainable Chemistry and Engineering*, *5*(9), 8089-8096. https://doi.org/10.1021/acssuschemeng.7b01708

ACS Sustainable Chemistry & Engineering
Research Article
pubs.acs.org/journal/ascecg

Electrochemical Behavior of Neodymium and Formation of Mg–Nd Alloys in Molten Chlorides

Zhongsheng Hua,*[†,‡] Huan Liu,[†] Jian Wang,[†] Jiwen He,[†] Saijun Xiao,[†,‡] Yanping Xiao,[†,§] and Yongxiang Yang[†,§]

[†] School of Metallurgical Engineering, Anhui University of Technology, Maxiang Road, Ma'anshan 243032, China

[‡] Key Laboratory of Metallurgical Emission Reduction & Resources Recycling, Anhui University of Technology, Ministry of Education, 59 Hudong Road, Ma'anshan 243002, China

[§] Department of Materials Science and Engineering, Delft University of Technology, Mekelweg 2, 2628 CD Delft, The Netherlands

Supporting Information

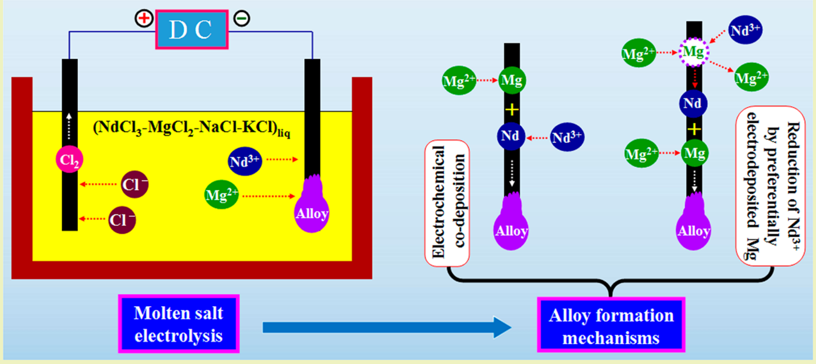

ABSTRACT: The electrochemical behavior of Nd(III) and its coreduction with Mg(II) were investigated on a molybdenum electrode at 1023 K in eutectic NaCl–KCl melts. The results indicate that the reduction of $NdCl_3$ in NaCl–KCl melts is a one-step process with three electrons exchanged, and the reaction is an irreversible diffusion-controlled process at low scan rate with the calculated diffusion coefficient of about 6.8×10^{-5} cm^2 s^{-1}. After $MgCl_2$ is introduced to the melts, the reduction of Nd(III) takes place at a more positive potential value due to the formation of Mg–Nd intermetallic compounds through electrochemical co-deposition and chemical reduction of Nd(III) ions by preferentially deposited Mg. The solid intermetallic compounds of Mg_3Nd, Mg_2Nd, and MgNd observed in open circuit chronopotentiometry curves are transformed to thermodynamically more stable Mg-rich phases of $Mg_{12}Nd$ and $Mg_{41}Nd_5$ when potentiostatic electrolysis at −2.10 V. It has been confirmed by X-ray diffraction and SEM-EDS microscopy that the cathodic deposits are composed of Mg, $Mg_{12}Nd$, $Mg_{41}Nd_5$, and Nd. The present results confirm that it is an effective method for recycling of neodymium from waste NdFeB magnets by means of electrochemical formation of Mg–Nd alloys from $NaCl\text{–}KCl\text{–}MgCl_2\text{–}NdCl_3$ melts.

KEYWORDS: *Electrochemical behavior, Co-deposition, Mg–Nd alloys, Formation mechanism, Melts*

INTRODUCTION

Nowadays, rare earth (RE) elements are playing an essential role in many highly functional materials such as permanent magnets, fluorescent powders, hydrogen storage alloys, catalysts, optical glass, etc.[1] Particularly, the demand and consumption for NdFeB permanent magnets have dramatically increased because of their extensive applications in computer hard disk drives (HDDs), cellular phones, motors in hybrid and electric vehicles ((H)EVs), and wind turbines owing to superior magnetic properties.[2] Consequently, RE metals are called key-enablers of modern technologies,[3,4] especially in the transition to a green economy.[1]

As the promotion and increasing application of new-energy vehicles such as HEVs and EVs throughout the world increases, the demand for Nd and Dy, will continue to increase steadily in the near future. However, we all have acknowledged the fact that China produced most of the world's RE elements over the past few decades, even though it currently has less than 37% of the RE reserves.[5,6] Owing to the scarcity, there is a growing concern that the world may soon encounter a shortage of more critical REs. Typically, NdFeB permanent magnets contain about 30 mass % RE elements mainly composed of Nd, as well as a small amount of Pr, Dy, and/or Tb.[2] To mitigate the RE supply risk, recycling of spent NdFeB permanent magnets has received increasing attention. At an industrial scale, in-plant magnet NdFeB scrap is recovered by hydrometallurgical

Received: May 30, 2017
Revised: July 27, 2017
Published: August 8, 2017

DOI: 10.1021/acssuschemeng.7b01708
ACS Sustainable Chem. Eng. 2017, 5, 8089–8096

technology, although it involves several drawbacks such as complicated processing steps, high consumption of chemicals and clean water, and generation of waste acid and effluent.[7] Thus, some pyrometallurgical recycling routes have been proposed.[8−11] However, they are still in laboratory scale currently and cannot meet the industrial requirements.

A simple and environmentally friendly recycling technology has been proposed by the authors.[2,12] The process consists of two main processing steps: (1) selective chlorination of REs with molten $MgCl_2$ and (2) direct electrolysis of the dissolved $RECl_3$ in molten chlorides to prepare an Mg−Nd based alloy. According to our previous work, RE metals (Nd, Pr, and Dy) in NdFeB magnet scrap can be extracted by the selective chlorination of molten $MgCl_2$ and transform into RE chlorides.[12] Because the standard electrode potential of RE is relatively close to that of Mg,[13−17] $NdCl_3$ in the obtained molten salts can be recovered directly as Mg−Nd-based alloys, which can be used as the master alloys or to prepare pure RE and Mg metals via evaporation.[11] To date, molten salts electrolysis is still the main method for industrial production of pure aluminum, magnesium, and most of the rare earth metals and has also been proposed to produce Mg−RE and Mg−Li−RE alloys.[13−15] Currently, most Mg−RE alloy is prepared via vacuum melting using pure Mg and RE metals as raw materials either in the laboratory or in industry.[13] It should be noticed that pure RE metals are difficult to extract and separate due to their chemical similarity, and thus, they are extremely expensive. Therefore, production of Mg−Nd-based alloys by direct electrochemical coreduction of RE salts together with Mg salts in the obtained chloride melts provides a unique opportunity for waste NdFeB magnet recycling for environmental and economic benefits.

Although reduction behavior of Nd(III) and formation of Mg−Nd alloys have been investigated in several studies,[16−18] the electrochemical behavior of Nd(III) and its coreduction with Mg(II) in molten NaCl−KCl eutectic, especially aimed at recycling neodymium from NdFeB scrap, have not been reported in the current literatures.[19] As part of a series of fundamental studies for developing a total recycling route,[12] the present article reports the electrochemical behavior of Nd(III) and production of Mg−Nd alloys in eutectic NaCl−KCl melts with an emphasis on the alloy formation mechanism, which is the necessary information for developing a novel NdFeB recycling technology via molten salt chlorination and electrolysis.

EXPERIMENTAL SECTION

Preparation of Electrolyte Melts. A mixture of NaCl−KCl salt with the eutectic composition of NaCl:KCl = 50.6:49.4 mol % was selected as the starting electrolyte due to its high thermal stability and good electrical conductivity, the natural abundance of sodium and potassium, and their comparatively stable electrode potential vs the Ag/AgCl reference electrode. The analytical reagents NaCl (>99.5% certified purity) and KCl (>99.5% certified purity) were first dried under vacuum for more than 72 h at 473 K to remove excess water and then fused in an alumina crucible (99.5 wt % Al_2O_3) in an electric furnace. Metal cation impurities in the NaCl−KCl melt were removed by pre-electrolysis at −2.10 V for 3 h. Anhydrous $MgCl_2$ (99.9%) and $NdCl_3$ (99.6%) were added directly into the melts as the source for Mg(II) and Nd(III) ions, respectively. All the experiments were performed in an inert atmosphere by purging with purified Ar gas at a rate of approximately 30 mL·min^{-1}.

Electrochemical Apparatus and Electrodes. Cyclic voltammetry, open circuit chronopotentiometry, and potentiostatic electrolysis were performed using PARSTAT 2273 electrochemical workstation (Ametek Group Co., American) with the PowerSuite software package. A conventional three-electrode cell was used for all the electrochemical measurements. A silver wire (99.99% purity with 1 mm in diameter) immersed in a solution of AgCl (1 wt %) in NaCl−KCl eutectic melts contained in a mullite tube (o.d. 6 mm × i.d. 4 mm × length 550 mm) was used as the reference electrode. All potentials were referred to this Ag^+/Ag couple in this study. A spectral pure graphite rod (6 mm in diameter) was employed as the counter electrode. A molybdenum wire (99.99% purity) of 1.0 mm in diameter served as the working electrode. The molybdenum wire was polished thoroughly using SiC paper followed by ultrasonic cleaning in ethanol (99.7% purity) prior to use. The active electrode surface area was calculated after each experiment by measuring the immersion depth of the electrode in the melts.

Electrolysis and Characterization of the Mg−Nd Alloy Product. The samples of Mg−Nd alloys were prepared by potentiostatic electrolysis at 1023 K. After the electrolysis, the cathodic product was cooled gradually to room temperature inside the furnace under an argon atmosphere and mechanically extracted from the melts. All Mg−Nd alloy samples were first immersed in ethylene glycol (99.5% purity) to remove the deposited salts and then ultrasonically cleaned in acetone (99.5% purity). Finally, they were embedded in acrylic resin and polished with SiC paper (#220, #400, #1000, and #1500) followed by ultrasonic cleaning in ethanol before being subjected to analysis. The crystal structures of alloys were analyzed by XRD (D8 Advance, Bruker axs) using the monochromatic target of Cu Kα. The microstructure was observed with SEM (SSX-550, Shinadzu Corporation), and the microzone chemical analysis was performed simultaneously with SEM using energy dispersive X-ray spectroscopy (EDS).

RESULTS AND DISCUSSION

Electrochemical Behavior of Nd(III) Ions. Figure 1 represents the cyclic voltammograms obtained on a molybdenum electrode in the NaCl−KCl eutectic melts before and after the addition of $NdCl_3$ at 1023 K. The dotted line in Figure 1 shows the typical cyclic voltammogram curve of the pure NaCl−KCl melts. The cathodic peak A at approximately −2.20 V and the corresponding anodic peak A′ in the reverse scan direction are attributed to the deposition and dissolution of sodium. Except for the cathodic/anodic signals A/A′, no other additional peaks exist in the electrochemical window and thus identifies the applicability of the NaCl−KCl melts for our

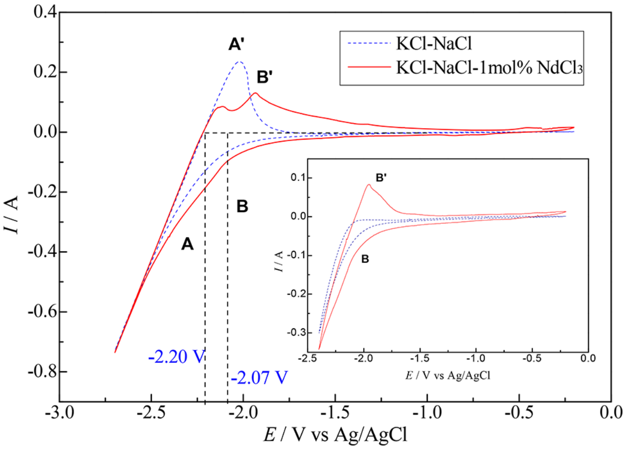

Figure 1. Cyclic voltammograms of the NaCl−KCl eutectic melts before (dotted line) and after (solid line) the addition of $NdCl_3$ (1 mol %) on a molybdenum electrode (S = 0.322 cm^2) with different inversion potentials. T = 1023 K; scan rate = 0.10 V s^{-1}.

investigations. After the addition of $NdCl_3$ (solid line), the current of the cathodic signal increases obviously, which is ascribed to the overlap of Nd and Na formation on the inert electrode due to their close deposition potentials. This phenomenon has also been detected by Tang et al. in the electrochemical fabrication of Mg−Pr alloys.[13] In the positive-going scan, a new anodic peak B′, which is attributed to the dissolution of Nd, is observed. At the same time, the current of anodic signal for Na decreases remarkably. This illustrates that the mass of deposited Na was reduced because a portion of the current was assigned for Nd reduction in the negative-going scan. To confirm the formation of Nd metal, we adjusted the cathodic terminal of the curves (see inset photo in Figure 1), which shows that only small quantity of Na deposits in the negative-going scan to −2.40 V in blank NaCl−KCl melts. When $NdCl_3$ is introduced into the melts, the cathodic current increases at around −2.07 V, and the oxidation peak shows a much higher amplitude in the reverse anodic scan. It can be inferred that the unnoticeable cathodic signal B at approximately −2.07 V, whose potential is slightly positive to the formation potential of Na, is attributed to the deposition of Nd metal. Moreover, apart from the signal couple A/A′ and B/B′, there are no other additional peaks in cyclic voltammograms, and thus, it is possible that Nd metal can be deposited in a single step though direct reduction of Nd(III) ions into Nd(0) on a molybdenum electrode. This result is similar to that reported by Zing et al.[20]

Furthermore, the reversibility of the redox reaction of Nd(III)/Nd(0) was evaluated over a wide scan rate range from 0.05 to 0.40 V s^{-1}. As shown in Figure 2a, with increasing scan rate, the cathodic/anodic signal couple B/B′ which corresponds to the deposition and dissolution of Nd shifts slightly. For a reversible electrode reaction, ΔE_p, the absolute difference value between anodic and cathodic peak potentials ($|E_{pa} - E_{pc}|$), should have a value of 0.0676 V ($2.3RT/nF$) for a three-electron reaction at 1023 K, independent of scan rate. It is shown in Figure 2a that the ΔE_p increases with increasing scan rate. Therefore, the deposition/dissolution reaction of Nd on the molybdenum electrode in the NaCl−KCl system is considered to be irreversible. Meanwhile, peak current (I_p) for the deposition/dissolution of Nd increases with scan rate (v). Based on the results from Figure 2a, the correlation of the cathodic peak current to the square root of the scan rates was determined and shown in Figure 2b. At low scan rate, it shows a near linear relationship, indicating that the electrode reaction is a diffusion controlled process. The diffusion coefficient (D) of Nd (III) ions in this investigated reaction system can be estimated using the Berzins−Delahay equation for a soluble−insoluble couple according to the theory of linear sweep voltammetry:[21]

$$I_p = -0.6105SC_0(nF)^{3/2}D^{1/2}v^{1/2}(RT)^{-1/2} \quad (1)$$

where S corresponds to the electrode surface area (cm^2), C_0 represents the solute concentration (mol cm^{-3}), n is the number of exchanged electrons, F denotes the Faraday constant (96,485C mol^{-1}), D is the diffusion coefficient (cm^2 s^{-1}), v designates the potential scanning rate (V s^{-1}), R is the universal gas constant (8.314 J mol^{-1} K^{-1}), and T is the absolute temperature (K). The diffusion coefficient of Nd(III) ions is calculated to be 6.8×10^{-5} cm^2 s^{-1} from the slope of the line in Figure 2b by eq 1.

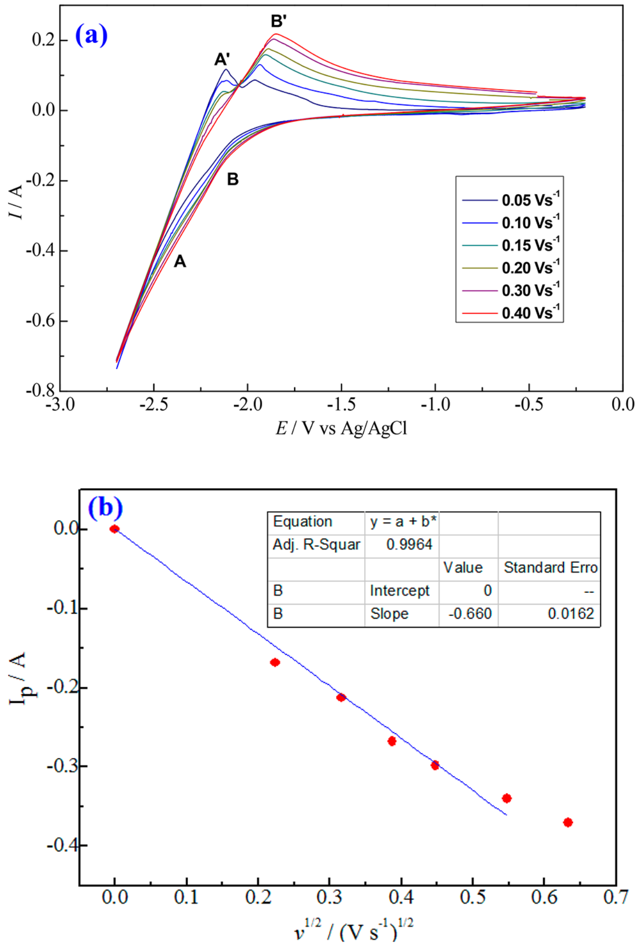

Equation	y = a + b*		
Adj. R-Squar	0.9964		
		Value	Standard Erro
B	Intercept	0	--
B	Slope	-0.660	0.0162

Figure 2. (a) Cyclic voltammograms of $NaCl-KCl-NdCl_3$ (1 mol %) melts on a molybdenum electrode ($S = 0.322$ cm^2) with different scan rates at 1023 K. (b) Plot of the cathodic peak current as a function of the square root of the scan rate.

It can be seen that only two couples of cathodic/anodic signals are observed from cyclic voltammograms and Nd deposits prior to Na in $NaCl-KCl-NaCl_3$ melts. In order to further validate the cathodic potential corresponding to the deposition of Nd, which is fairly close to that of Na detected by cyclic voltammograms, open circuit chronopotentiometry was adopted to identify the cathodic potential for Nd deposition and to confirm that Nd metal does not react with Na metal to form alloys. For this investigation, a thin layer specimen was first deposited on a molybdenum electrode by potentiostatic electrolysis at −2.50 V vs Ag/AgCl for a short period. Then, the open-circuit potential of the electrode versus time is registered, as shown in Figure 3. Curve (a) indicates the open circuit chronopotentiogram obtained in a blank NaCl−KCl eutectic at a molybdenum electrode by pre-electrolysis at −2.50 V for 20 s. Obviously, there is only one potential plateau at around −2.20 V, which is ascribed to the deposition of Na metal on molybdenum electrode. After the addition of 0.33 mol % $NdCl_3$, another new potential plateau at −2.07 V appears in curve (b), which should be attributed to the equilibrium potential of Nd(III)/Nd system. When more $NdCl_3$ was added to the melts, potential plateau 2 lasts for a longer time, while the duration of potential plateau 1 decreases, as shown in curves (c) and (d), because Nd deposition occurs preferentially during electrolysis process. Thus, there are less Na deposits

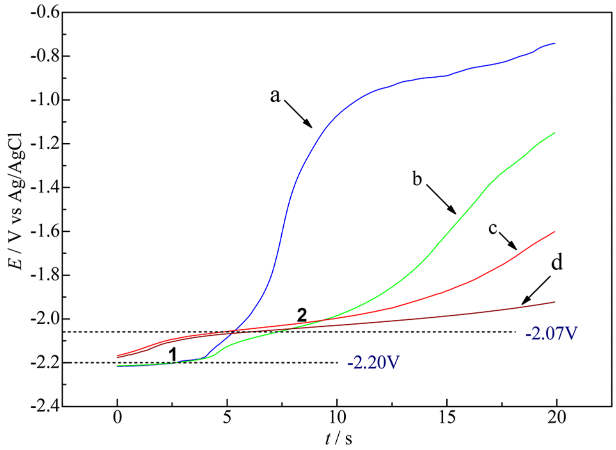

Figure 3. Open-circuit potential transient curves obtained on molybdenum electrode after electrodepositing at −2.50 V vs Ag/AgCl for 20 s at 1023 K: (a) in a blank NaCl−KCl eutectic melts, (b) in NaCl−KCl eutectic melts contaning 0.33 mol % $NdCl_3$, (c) in NaCl−KCl eutectic melts containing 0.67 mol % $NdCl_3$, and (d) in NaCl−KCl eutectic melts containing 1 mol % $NdCl_3$.

when $NdCl_3$ was introduced to the melts, and meanwhile, the amount of Na metal deposited on the electrode decreases with an increased concentration of $NdCl_3$ in the melts under the given electrolysis conditions. Furthermore, no other potential plateaus have been detected in curves (b), (c), and (d), indicating that Nd does not form alloys with Na.

Preliminary Discussions on Electrochemical Co-Deposition. The results obtained in the previous section indicate that Nd metal could be deposited on an inert electrode in a single step through reduction of Nd(III) directly into Nd(0) with three electrons exchanged. Theoretically, Nd(III) ions could also be reduced simultaneously with Mg(II) ions to form Mg−Nd alloys via electrochemical co-deposition in molten chlorides on an inert electrode owing to their similar standard electrode potentials. The electrochemical co-deposition is a simultaneous reduction of two or more metallic ions on an inert electrode to form alloys. However, the so-called co-deposition does not refer to the simultaneous reduction of metallic ions at the same potential. As for Nd(III) and Mg(II) ions in the NaCl−KCl system, to realize the simultaneous reduction at the same potential, the activity of Nd(III) and Mg(II) ions should satisfy the following relationship according to Nernst equation:

$$a_{\mathrm{Nd}^{3+}} = a_{\mathrm{Mg}^{2+}}^{3/2}\exp\frac{3F(E^{\Theta}_{\mathrm{Mg}} - E^{\Theta}_{\mathrm{Nd}})}{RT} \qquad (2)$$

where $a_{\mathrm{Nd}^{3+}}$ and $a_{\mathrm{Mg}^{2+}}$ denote the activity of Nd(III) and Mg(II) ions in NaCl−KCl melts, respectively, F denotes the Faraday constant (96,500C mol^{-1}), R is the universal gas constant (8.314 J mol^{-1} K^{-1}), T is the absolute temperature (K), and E^{Θ}_{Nd} and E^{Θ}_{Mg} designate the theoretical decomposition voltage of $NdCl_3$ and $MgCl_2$ (V), respectively. According to the theoretical decomposition voltage of $NdCl_3$ and $MgCl_2$ at 1023 K, $a_{\mathrm{Nd}^{3+}}$ must be roughly 4.9×10^3 times larger than $a_{\mathrm{Mg}^{2+}}$ calculated from eq 2. That is practically impossible during electrolysis. Actually, the principle of the co-deposition process is that a more noble metal allows the more reactive ones to be reduced at a potential more positive than that for the deposition of a pure metal, provided that they can form intermetallic compounds.[22]

Mg−Nd Alloy Formation Mechanism. Typical cyclic voltammograms of NaCl−KCl−$MgCl_2$ (2 mol %) (dotted line) and NaCl−KCl−$MgCl_2$ (2 mol %) −$NdCl_3$ (1 mol %) melts (solid line) obtained on a molybdenum electrode are shown in Figure 4. Compared with the blank NaCl−KCl melts (Figure 1), a new pair of signals, C/C′ is observed at around −1.80/−1.40 V in NaCl−KCl−$MgCl_2$ (2 mol %) melts. The cathode signal C with a steep rise at −1.80 V is attributed to the reduction of Mg(II) ions, and the corresponding anode signal C′ is related to the oxidation of Mg metal. In NaCl−KCl−$MgCl_2$ (2 mol %) −$NdCl_3$ (1 mol %) melts, apart from the reduction signal C assigned for Mg(II) ions, the cathodic current shows an obvious increase at approximately −1.88 V. The deposition potential of pure Nd metal on a molybdenum electrode in molten chlorides is −2.07 V, so that the cathode signal D could be related to the formation of Mg−Nd alloys via the underpotential deposition of Nd(III) ions on predeposited Mg. According to the phase diagram of Nd and Mg (see Figure S1 in Supporting Information),[23] five Mg−Nd intermetallics could be formed on a molybdenum electrode at 1223 K. However, only one cathode signal corresponding to the formation of intermetallic Mg−Nd has been detected. The absence of other Mg−Nd intermetallics could be due to their similar deposition potentials to that of signal D, and the very slow formation of these compounds. A similar phenomenon has also been detected in investigating Mg−Tm and Sm−Al alloys by cyclic voltammograms.[24,25] In the anodic potential scan direction, an insignificant anodic signal D′, as shown in the inset in Figure 4, a little more negative than signal C′, is present, which could be related to subsequent dissolution of Mg−Nd intermetallics.

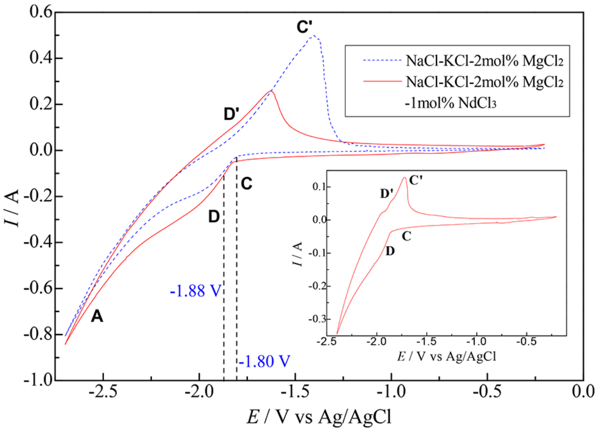

Figure 4. Cyclic voltammograms of NaCl−KCl−$MgCl_2$ (2 mol %) (dotted line) and NaCl−KCl−$MgCl_2$ (2 mol %) −$NdCl_3$ (1 mol %) melts (solid line) obtained on a molybdenum electrode. T = 1023 K; scan rate = 0.10 V s^{-1}.

Interestingly, the current of cathodic signal C is almost unchanged, but its corresponding anodic current (signal C′) markedly decreases when $NdCl_3$ is introduced into NaCl−KCl−$MgCl_2$ melts. It indicates that in the positive-going scan, the mass of Mg(0) oxidized to Mg(II) decreases after the addition of $NdCl_3$ to the melts. This is probably because a portion of predeposited Mg is consumed for the reduction of Nd(III) ions through the following reaction:

$$3\mathrm{Mg} + 2\mathrm{Nd}^{3+} \rightarrow 2\mathrm{Nd}\ (\mathrm{in\ Mg{-}Nd}) + 3\mathrm{Mg}^{2+} \qquad (3)$$

DOI: 10.1021/acssuschemeng.7b01708
ACS Sustainable Chem. Eng. 2017, 5, 8089−8096

It is particularly noteworthy that the reduction of Nd(III) to elemental Nd by Mg should not take place thermodynamically. Nevertheless, Nd in the reduction product is not elemental substance but is in Mg−Nd alloys. The activity of Nd in Mg−Nd alloys is much smaller than that of pure Nd metal, and thus, the above reaction could proceed spontaneously.[17] In fact, this viewpoint has also been approved in terms of the Tm(III) reduction on Mg and Sm(III) reduction on Al.[24,25] In addition, the oxidation potential of Mg(0) shifts toward a more negative value, as clearly shown in Figure 4, which likely results from the adjacent shoulder D′ corresponding to the dissolution of underpotentially deposited Mg−Nd alloys. Therefore, it can be concluded that the co-depostion principle of Mg−Nd alloys is a combination of electrochemical coreduction of Nd(III) with Mg(II) and chemical reduction of Nd(III) ions by predeposited Mg.

The results from the above cyclic voltammetry study are not sufficient to identify the underlying intermetallic compounds, and hence, the open circuit chronopotentiometry is conducted to investigate the possible formation and dissolution processes of Mg−Nd alloys. Figure 5 illustrates the open circuit chronopotentiometry curves obtained on a molybdenum electrode ($S = 0.322$ cm^2) after pre-electrolysis at a potential of −2.50 V for 100 s in NaCl−KCl−$MgCl_2$ (2 mol %) −$NdCl_3$ (1 mol %) melts at 1023 K. The evolution of the potential consists of successive plateaus with increasing potential, and each plateau represents an electrochemial equilibrium in the coexisting state of the two solid intermetallic compounds.[26] Originally, the potential staying at around −2.20 V (plateau 1) is related to the deposition of Na metal on molybdenum electrode and corresponds to the Na(I)/Na redox couple. Afterward, plateau 2 at around −2.07 V is associated with the Nd(III)/Nd(0) system. Plateau 3 occurring at approximately −1.81 V with a long step time is ascribed to Mg(II)/Mg redox couple. The results are in a good agreement with those investigated by cyclic voltammetry technique. Apart from these three potential plateaus, the chronopotentiogram also consists of three plateaus I, II, and III, which can be interpreted as the formation of Mg−Nd alloys. A very similar phenomenon has also been reported in electrochemical formation of Al−Ce alloy in molten chlorides.[27]

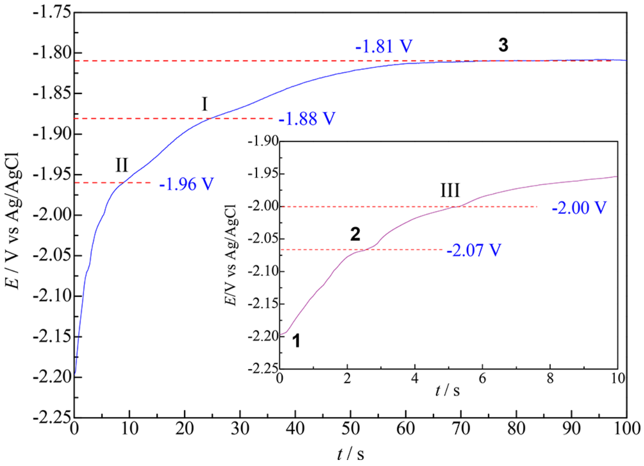

Figure 5. Open-circuit potential transient curve for molybdenum electrode after electrodepositing at −2.50 V vs Ag/AgCl for 100 s at 1023 K in the NaCl−KCl−$MgCl_2$ (2 mol %) −$NdCl_3$ (1 mol %) melts.

According to the Mg−Nd phase diagram,[23] three solid intermetallics are present in the binary system at 1023 K. The potential is dictated by the difference of the neodymium activity in the electrolyte and at the surface of Mg−Nd alloys. The neodymium concentration decreases at the surface of the electrode as it diffuses into predeposited Mg. When a biphasic equilibrium in the solids establishes at the surface of the electrode, the neodymium activity is identical in each phase and maintains constant, which consequently results in a constant potential (plateau) for a given time. Plateau III at −2.00 V is related to intermetallic MgNd because it is the compound containing the highest concentration of Nd and thus is the last to be reduced. Therefore, plateaus I, II, and III could be considered corresponding to the coexisting states of Mg_3Nd and Mg, Mg_2Nd and Mg_3Nd, and MgNd and Mg_2Nd, respectively. The possible equilibrium reactions are summarized in Table 1. From open circuit chronopotentiometry, the electrochemical co-deposition process of Mg−Nd alloys could include two consecutive steps described as follows:

Table 1. Potential Corresponding to Possible Equilibrium Reactions

Plateau	Equilibrium potential (V)	Reaction	Atomic ratio (x:y) of dissolution MgxNdy
I	−1.88	$Mg_3Nd-3e^- \leftrightarrow 3Mg+Nd^{3+}$	3:1
II	−1.96	$3Mg_2Nd-3e^- \leftrightarrow 2Mg_3Nd+Nd^{3+}$	2:1
III	−2.00	$2MgNd-3e^- \leftrightarrow Mg_2Nd+Nd^{3+}$	1:1

$$xMg^{2+} + 2xe^- \rightarrow xMg \tag{4}$$

$$yNd^{3+} + xMg + 3ye^- \rightarrow Mg_xNd_y \tag{5}$$

The overall reaction can be written as follows:

$$xMg^{2+} + yNd^{3+} + (2x + 3y)e^- \rightarrow Mg_xNd_y \tag{6}$$

In fact, Mg(II) ions are preferentially reduced to pure metal on the inert electrode, and Nd(III) ions are subsequently reduced on Mg-coated electrode to form Mg−Nd alloys. In other words, the deposition of Nd(0) is essentially identical to the underpotential deposition on an active Mg cathode. Owing to the depolarization effect, compared with the deposition of pure Nd on a molybdenum electrode, coreduction of Nd(III) with Mg(II) allows for the deposition of Nd to occur at more positive potentials, as shown in Figures 4 and 5. This can be expressed from the following equilibrium potential of Nd/Mg_xNd_y system involved in eq 5:

$$E_{Nd^{3+}/Mg_xNd_y} = E_{Nd^{3+}/Nd} - \frac{RT}{3F}\ln[a_{Nd}\ (\text{in } Mg_xNd_y)] \tag{7}$$

where $E_{Nd^{3+}/Nd}$ designates the equilibrium potential of pure Nd element and a_{Nd}(in Mg_x Nd_y) denotes the activity of Nd in the intermetallic compound Mg_xNd_y. Since α_{Nd} (in Mg_x Nd_y) < 1, the relation $E_{Nd3^+/Mg_x Nd_y} > E_{Nd^{3+}/Nd}$ is evident. Moreover, the activities of Nd vary in different Mg−Nd intermetallic compounds, and thereby three potential plateaus (I, II, and III) corresponding to three different Mg−Nd intermetallic compounds appear in the chronopotentiogram.

Electrolysis and Characterization of Mg−Nd Alloys. According to the cathode potential previously determined by cyclic voltammetry and open circuit chronopotentiometry, potentiostatic electrolysis was carried out at −2.10 V on a molybdenum electrode at 1023 K for 10 h in the electrolyte containing eutectic NaCl−KCl melts with additional 2 mol % $MgCl_2$ and 1 mol % $NdCl_3$. Figure 6a shows the evolution of the cathodic current and the obtained alloys after washing. When the direct current was applied to the electrolyte, Mg(II) and Nd(III) ions were immediately reduced to form a monolayer of Mg−Nd alloys on the molybdenum electrode, and the resistance between the electrode and electrolyte decreased with time. The current rapidly rose up to −0.73 A in the initial stage of electrolysis. Afterward, the current tardily increased because the working surface area of the electrode was gradually enlarged with the deposition of Mg−Nd alloys. When an electrolysis time reached about 10,000 s, a sudden fluctuation occurred because of the drop-off of the deposited alloys possibly caused by the changes of surface tension and shrinkage of the liquid surface of Mg−Nd alloys. After continual electrolysis for about 9000 s, the current was maintained at around −0.89 A, which is attributed to the fact that the contributions of surface area enlargement and the depletions of Nd(III) and Mg(II) ions reach a balance. When the electrolysis has proceeded for 25,000 s, the current starts to decrease gradually because of the serious depletion of Mg(II) and Nd(III) ions in the melts. After electrolysis, the bulk alloys (see inset in Figure 6a) were obtained at the bottom of the melts beneath the working electrode. According to the subsequent XRD analysis, the experiment temperature is much higher than the melting point of the obtained alloys. The liquid drop of Mg−Nd alloys could spread out on the crucible bottom and thus solidify to an oblate bulk. Herein, the oblate shape could be ascribed to the fairly low melting point and favorable fluidity of Mg−Nd alloys under electrolysis temperature.

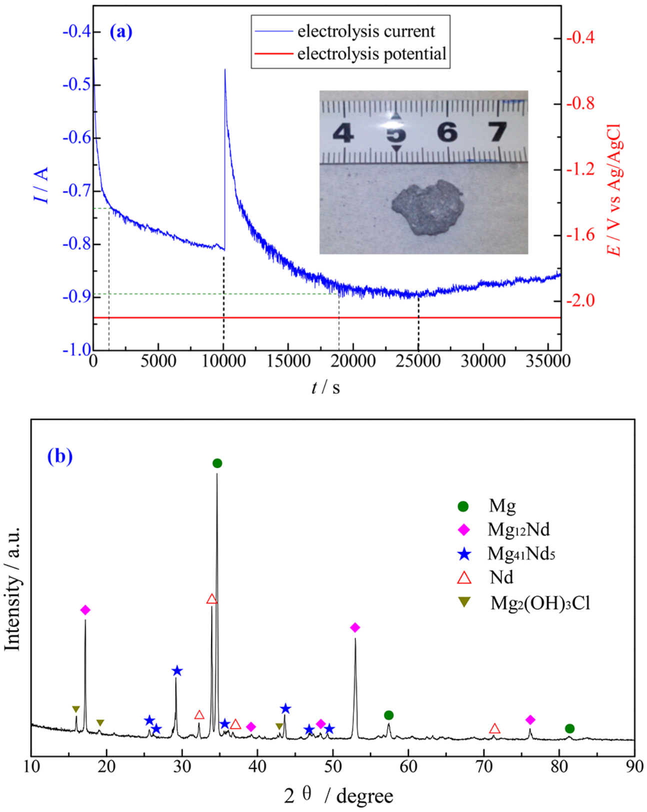

Figure 6. (a) Typical evolution of cathodic currents and potentials during electrolysis obtained on a molybdenum electrode (S = 0.322 cm^2) in eutectic NaCl−KCl melts containing 2 mol % $MgCl_2$ and 1 mol % $NdCl_3$. T = 1023 K. Inset photo: Mg−Nd alloys sample obtained by potentiostatic electrolysis. (b) X-ray diffraction analysis of the cathodic deposits obtained by potentiostatic electrolysis.

The XRD pattern of the alloys obtained by potentiostatic electrolysis is shown in Figure 6b. The observed peaks in the patterns are identified as Mg, $Mg_{12}Nd$, $Mg_{41}Nd_5$, Nd, and $Mg_2(OH)_3Cl$ phases. The peaks assigned for $Mg_2(OH)_3Cl$ are weak, and the formation of $Mg_2(OH)_3Cl$ may result from the hydrolysis reaction of residual $MgCl_2$ on the sample. Apart from Mg and Nd phases, two intermetallic compounds of $Mg_{12}Nd$ and $Mg_{41}Nd_5$ were also identified. Three intermetallic compounds corresponding to plateaus I, II, and III as analyzed based on the open-circuit potentiogram were not found in the obtained alloys. This could be due to the relatively low current density applied in the present experiment. The formation reactions of several Mg−Nd alloys, such as Mg_3Nd, Mg_2Nd, and MgNd, would be kinetically slow. In other words, Mg_3Nd, Mg_2Nd, and MgNd intermetallic compounds formed via coreduction quickly diffuse into the Mg metal, and the formation rate is much slower than the diffusion rate, which results in the transformation of these phases into the thermodynamically more stable Mg-rich phases of $Mg_{12}Nd$ and $Mg_{41}Nd_5$. A similar phenomenon has also been detected in electrochemical formation of Dy−Ni alloys.[7] In effect, molten Mg−Nd was produced in the electrolysis. When its density gets more than that of the melts with the diffusion of reduced Nd into the alloys, the liquid alloy falls down to the bottom of crucible. According to the phase diagram, when molten Mg−Nd alloy was cooled gradually to ambient temperature in the melts, it will produce $Mg_{41}Nd_5$ at around 650 °C and $Mg_{12}Nd$ at about 600 °C. The presence of $Mg_{12}Nd$ and $Mg_{41}Nd_5$ in cathodic deposits also confirms, in turn, that the generated alloys are liquid at the experimental temperature, and thus fall down to the bottom of the crucible.

To further examine the distribution of Nd and Mg elements in the obtained Mg−Nd alloys, microstructure and microzone chemical composition of the alloys were determined using SEM and EDS. Figure 7a shows the SEM image of the Mg−Nd alloys obtained by potentiostatic electrolysis at 1023 K. It can be seen that Mg−Nd alloys were predominantly distinguished by three zones (dark, gray, and bright). The results of EDS analysis of the zones labeled A, B, and C taken from three represented zones in Figure 7a indicate that the deposits are simply composed of Mg and Nd, as shown in Figure 7b−d. For zone A, the atomic ratio of Mg:Nd is about 15.3. Considering the measurement error, the dark zone in the alloys likely consists of $Mg_{12}Nd$ and Mg. The atomic ratio of Mg to Nd in zone B is close to 8:1, so that the gray part could be regard as the $Mg_{41}Nd_5$ phase. Around zone C, many different sizes of extremely bright spots, which discretionarily distribute on the surface of the alloys, could be ascribed to another new phase of pure Nd. The atomic ratio of Mg:Nd in zone C is roughly 3.7, and thus, the bright zone surrounded by some brighter spots is probably composed of $Mg_{41}Nd_5$ and Nd phases. The results are consistent with those from XRD analysis.

Based on cyclic voltammetry and open circuit chronopotentiometry investigations, the reduction process of Nd(III) and Mg(II) ions in molten NaCl−KCl salts could be considered to proceed in three steps: (1) Mg(II) ions are

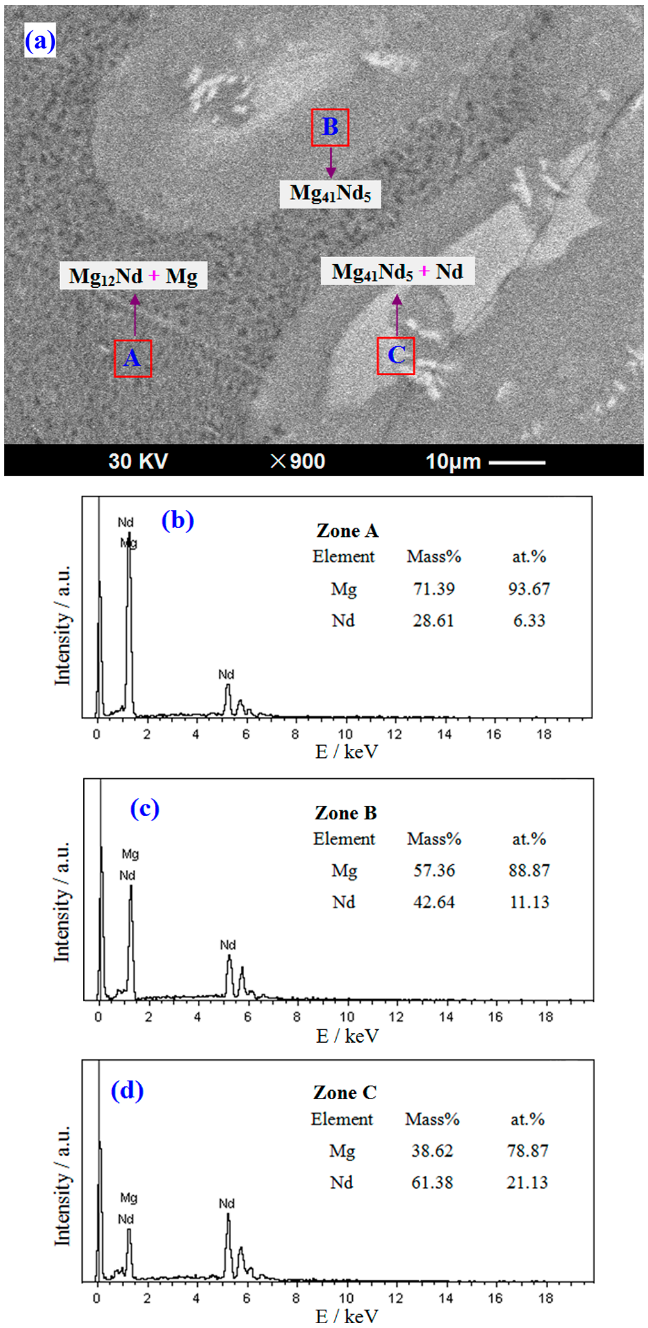

Figure 7. SEM image (a) and EDS analysis of the zones labeled A, B, and C taken from three represented zones (b–d) of Mg–Nd alloys by electrolysis at 1023 K from NaCl–KCl–$MgCl_2$ (2 mol %) –$NdCl_3$ (1 mol %) melts.

preferentially reduced to Mg(0) metal. (2) Nd(III) ions are then reduced on predeposited Mg to form Mg–Nd alloys via underpotential deposition and chemical reduction. (3) Finally, Nd(III) ions are reduced to Nd(0) metal at a more negative potential onto a Mg–Nd alloy surface. According to the results of XRD and SEM-EDS analysis, production of Mg–Nd alloys via electrochemical co-deposition with Mg at a more positive potential is an effective method to extract Nd from NaCl–KCl–$MgCl_2$–$NdCl_3$ melts. This proves that recycling of Nd from waste NdFeB magnets to form Mg–Nd alloys is technically feasible.

■ CONCLUSION

The electrochemical behavior of Nd(III) ions in NaCl–KCl eutectic melts with and without the addition of $MgCl_2$ on a molybdenum electrode at 1023 K was experimentally investigated by cyclic voltammetry and open circuit chronopotentiometry techniques in order to understand the formation mechanisms of Mg–Nd alloys. The results indicate that Nd(III) ions can be directly reduced to Nd metal at the potential of about −2.07 V (vs Ag/AgCl) on the inert electrode through a single step mechanism with three electrons exchanged in eutectic NaCl–KCl melts. The deposition/dissolution reaction of Nd on molybdenum electrode in NaCl–KCl system is considered to be an irreversible process and controlled by diffusion at low scan rate with a diffusion coefficient of Nd(III) ions estimated to be 6.8×10^{-5} cm^2 s^{-1}.

Cyclic voltammetry at 1023 K shows that the reduction potential of Nd(III) ions shifts toward a more positive value of about −1.88 V after the addition of $MgCl_2$ to the melts. Three plateaus present in open circuit chronopotentiometry between −1.88 and −2.07 V are probably attributed to the equilibrium reactions of three solid intermetallic compounds (Mg_3Nd, Mg_2Nd, and MgNd) at the experiment temperature. The reduction process of Nd(III) in NaCl–KCl–$MgCl_2$–$NdCl_3$ melts is likely the combination of underpotential deposition and magnesium reduction.

Mg–Nd alloys are obtanined by potentiostatic electrolysis at −2.10 V on molybdenum electrode in NaCl–KCl–$MgCl_2$–$NdCl_3$ melts at 1023 K for 10 h. During this process, it is thought that Mg(II) ions were preferentially reduced to Mg metal, followed by reduction of Nd(III) ions on the predeposited Mg through underpotential deposition and magnesium reduction, and finally, Nd(III) ions are reduced to Nd metal at a more negative potential. The obtained bulk alloys consists of four phases of Mg, $Mg_{12}Nd$, $Mg_{41}Nd_5$, and Nd. The formation reactions of the intermetallic compounds Mg_3Nd, Mg_2Nd, and MgNd would be kinetically slow, and the thermodynamically more stable Mg-rich phases of $Mg_{12}Nd$ and $Mg_{41}Nd_5$ are formed under the experiment conditions. These investigations demonstrate that electrochemical reduction of Nd(III) with Mg(II) to form Mg–Nd alloys in NaCl–KCl–$MgCl_2$–$NdCl_3$ melts is an effective method for recycling of neodymium from NdFeB magnet scrap.

■ ASSOCIATED CONTENT

Ⓢ Supporting Information

The Supporting Information is available free of charge on the ACS Publications website at DOI: 10.1021/acssuschemeng.7b01708.

Phase diagram of Mg–Nd. (PDF)

■ AUTHOR INFORMATION

Corresponding Author

*E-mail: huazs83@163.com. Phone: +86 555-2311571. Fax: +86 555-2311571.

ORCID

Zhongsheng Hua: 0000-0002-5984-1336

Notes

The authors declare no competing financial interest.

ACKNOWLEDGMENTS

This work was financially supported by the National Natural Science Foundation of China (51204002) and the Foundation of Key Laboratory of Metallurgical Emission Reduction & Resources Recycling, Ministry of Education, China (KF17-04). The authors are particularly grateful to Dr. Yonglin Yao for his kind help in data processing of this work.

REFERENCES

(1) Binnemans, K.; Jones, P. T.; Blanpain, B.; Van Gerven, T.; Yang, Y.; Walton, A.; Buchert, M. Recycling of rare earths: a critical review. *J. Cleaner Prod.* **2013**, *51*, 1−22.

(2) Hua, Z. Rare Earth Recycling from NdFeB. In *Encyclopedia of Inorganic and Bioinorganic Chemistry*; Atwood, D. A., Ed.; John Wiley & Sons: Chichester, U.K., 2016.

(3) Martinez, A. M.; Kjos, O.; Skybakmoen, E.; Solheim, A.; Haarberg, G. M. Extraction of rare earth metals from Nd-based scrap by electrolysis from molten slag. *ECS Trans.* **2013**, *50* (11), 453−461.

(4) Sprecher, B.; Kleijn, R.; Kramer, G. J. Recycling potential of neodymium: The case of computer hard disk drives. *Environ. Sci. Technol.* **2014**, *48* (16), 9506−9513.

(5) Kobayashi, S.; Kobayashi, K.; Nohira, T.; Hagiwara, R.; Oishi, T.; Konishi, H. Electrochemical formation of Nd−Ni alloys in molten LiF−CaF_2−NdF_3. *J. Electrochem. Soc.* **2011**, *158* (12), E142−E146.

(6) *Mineral Commodity Summaries*; U.S. Geological Survey, 2012.

(7) Kobayashi, S.; Nohira, T.; Kobayashi, K.; Yasuda, K.; Hagiwara, R.; Oishi, T.; Konishi, H. Electrochemical formation of Dy-Ni alloys in molten LiF−CaF_2−DyF_3. *J. Electrochem. Soc.* **2012**, *159* (12), E193−E197.

(8) Bian, Y.; Guo, S.; Jiang, L.; Liu, J.; Tang, K.; Ding, W. Recovery of rare earth elements from NdFeB magnet by VIM-HMS method. *ACS Sustainable Chem. Eng.* **2016**, *4* (3), 810−818.

(9) Mochizuki, Y.; Tsubouchi, N.; Sugawara, K. Selective recovery of rare earth elements from Dy containing NdFeB magnets by chlorination. *ACS Sustainable Chem. Eng.* **2013**, *1* (6), 655−662.

(10) Itoh, M.; Miura, K.; Machida, K. Extraction of rare earth elements from Nd-Fe-B magnet scraps by NH_4Cl. *Chem. Lett.* **2008**, *37* (3), 372−373.

(11) Xu, Y.; Chumbley, L. S.; Laabs, F. C. Liquid metal extraction of Nd from NdFeB magnet scrap. *J. Mater. Res.* **2000**, *15* (11), 2296−2304.

(12) Hua, Z.; Wang, J.; Wang, L.; Zhao, Z.; Li, X.; Xiao, Y.; Yang, Y. Selective extraction of rare earth elements from NdFeB scrap by molten chlorides. *ACS Sustainable Chem. Eng.* **2014**, *2* (11), 2536−2543.

(13) Tang, H.; Yan, Y. D.; Zhang, M. L.; Li, X.; Han, W.; Xue, Y.; Zhang, Z.; He, J. H. Fabrication of Mg−Pr and Mg−Li−Pr alloys by electrochemical co-reduction from their molten chlorides. *Electrochim. Acta* **2013**, *107*, 209−215.

(14) Xue, Y.; Yan, Y. D.; Zhang, M. L.; Han, W.; Zhang, Z. J. Electrochemical formation of Mg−Li−Y alloys by co-deposition of magnesium, lithium and yttrium ions in molten chlorides. *J. Rare Earths* **2012**, *30*, 1048−1054.

(15) Han, W.; Wang, F. L.; Tian, Y.; Zhang, M. L.; Yan, Y. D. Electrochemical formation of Mg−Li−Sm alloys by codeposition from LiCl−KCl−$MgCl_2$−$SmCl_3$ molten salts. *Metall. Mater. Trans. B* **2011**, *42* (6), 1376−1382.

(16) Zhang, D. P.; Fang, D. Q.; Wang, J.; Tang, D. X.; Lu, H. Y.; Zhao, L. S.; Meng, J. Preparation of magnesium-rare earth master alloy using electrowinning method with subsidence cathode. *Mater. Sci. Forum* **2005**, *488−489*, 235−238.

(17) Liu, X. D.; Qiu, X.; Sun, W.; Tian, Z.; Meng, J.; An, J. Research on parameters and mechanism of preparation of Mg-RE (Rare Earth) alloy in a magnesium-electrolyzed electrolyzer. *J. Chinese Rare Earth Society* **2013**, *31* (2), 482−487 (In Chinese).

(18) Mediaas, H.; Tkatcheva, O.; Dracopoulos, V.; Papatheodorou, G. N.; Kipouros, G. J.; Østvold, T. Solubilities and raman spectra of NdOCl in some chloride melts of interest for the electrowinning of magnesium from its oxide. *Metall. Mater. Trans. B* **2000**, *31* (4), 631−639.

(19) Wang, J.; Hua, Z.; Ma, H.; Fan, Y.; Wang, L. Research progress on preparation of rare earth magnesium alloys by molten salt electrolysis. *Chinese Rare Earths* **2017**, *38* (2), 100−113 (In Chinese).

(20) Zing, C. A.; Su, M.; Du, S.; Tang, D. Study of the deposition mechanism of neodymium on an iron consumable cathode and a molybdenum unconsumable cathode in NaCl + KCl (1:1) in the temperature range 700−850 °C. *J. Electroanal. Chem. Interfacial Electrochem.* **1989**, *263* (2), 399−413.

(21) Bard, A. J.; Faulkner, L. R. *Electrochemical Methods: Fundamentals and Applications*, 2nd ed.; John Wiley & Sons: New York, 2002.

(22) Su, L. L.; Liu, K.; Liu, Y. L.; Wang, L.; Yuan, L. Y.; Wang, L.; Li, Z. J.; Zhao, X. L.; Chai, Z. F.; Shi, W. Q. Electrochemical behaviors of Dy (III) and its co-reduction with Al (III) in molten LiCl-KCl salts. *Electrochim. Acta* **2014**, *147*, 87−95.

(23) Binary Alloy Phase Diagrams, second ed. ASM International, 1996.

(24) Li, X.; Yan, Y. D.; Zhang, M. L.; Tang, H.; Ji, D. B.; Han, W.; Xue, Y.; Zhang, Z. J. Electrochemical reduction of Tm on Mg electrodes and co-reduction of Mg, Li and Tm on W electrodes. *Electrochim. Acta* **2014**, *135*, 327−335.

(25) Castrillejo, Y.; Fernández, P.; Medina, J.; Hernández, P.; Barrado, E. Electrochemical extraction of samarium from molten chlorides in pyrochemical processes. *Electrochim. Acta* **2011**, *56*, 8638−8644.

(26) Nourry, C.; Massot, L.; Chamelot, P.; Taxil, P. Formation of Ni-Nd alloys by Nd (III) electrochemical reduction in molten fluoride. *J. New Mater. Electr. Sys.* **2007**, *10* (2), 117−122.

(27) Zhang, M.; Wang, H.; Han, W.; Zhang, M.; Li, Y.; Wang, Y.; Xue, Y.; Ma, F.; Zhang, X. Electrochemical extraction of cerium and formation of Al-Ce alloy from CeO_2 assisted by $AlCl_3$ in LiCl-KCl melts. *Sci. China: Chem.* **2014**, *57* (11), 1477−1482.

NOTE ADDED AFTER ASAP PUBLICATION

This paper was published ASAP on August 21, 2017, with an error in Figure 6a. The corrected version was published ASAP on August 25, 2017.